Design of Two-Dimensional Photonic Crystal Based Biosensors for Abnormal Tissues Analysis

A Asuvaran (asuvaran@gmail.com)
University College of Engineering Pattukkottai https://orcid.org/0000-0002-8425-2971
G Elatharasan
University College of Engineering Pattukkottai

Research Article

Keywords: Minimally Invasive Surgery, Photonic Crystal, Bio-sensor, Refractive Index,

Posted Date: June 22nd, 2021

DOI: https://doi.org/10.21203/rs.3.rs-628354/v1

Abstract

The recognition of different classifications of brain irregular tissues is an incredible test in robot-helped Minimally Invasive Surgery (MIS) that includes connection with the tissues. In this paper, an optical sensor was designed in order to assess the Refractive Index (RI) of various brain tissues while the robotic surgery is performed. This research work is based on the 2-Dimensional (2D) Photonic Crystal (PC) bio-sensor powered by electromagnetic radiation. It reaches the range from UV to IR and is deeply intended to profoundly touch the changes in the refractive index of different tissues. Due to the fact that the refractive index of the abnormal tissues is very different from the normal tissues, the sensor can easily be distinguished the tumors, cancer-infected brain tissues, and normal brain tissues. As a result, the sensor exhibits a different range of frequency, wavelength and amplitude spectra which respond to the small changes that occur in the refractive index of the brain tissue.

1. Introduction

Research on abnormal brain tissue is very essential and challenging today because it can cause serious human health issues. Although there are many surgical techniques for brain surgery, Minimally Invasive Surgery (MIS) surgical techniques have been used for research work because of their unique features and the most feasible one. One of the most notable recent surgical techniques is MIS, which is used do the surgery the internal organs of the human body with minimal damage. The endoscopic camera and surgical instruments are inserted into the human body either by natural orifices or by Punctures which were designed by the surgeon.

The interior organs picture and the total function of the human body can be viewed on the screen by means of the camera. The specialist surgeon needs to understand the tissue characteristics by the feeling in that way the construction are implanted. The presence of vessels and channels which are by and large canvassed in connective tissue ought to be felt rather than seen to avoid hurt. In general, the channel and vessel are in the connective tissue should avoid harm to them. The sensation of touch is a crucial portion of our perspective on the world. Present endoscopic grasper have a rigid tooth grasper for grasping slippery tissues if the grasper equipped with a sensor, then tactile information can be displayed to the surgeon.

If the current endoscopic grasper is designed with the use of a sensor to analyze the slippery tissues, then the information about the tactile can be easily informed to the surgeon. Brain tumors are one of the pediatric cancer disease (15–20%) and cause serious death related to cancer diseases between the age of 15 to 29 years [1, 2].Minimally Invasive Endoscopic Intra ventricular (MIES) surgery is one of the robot-assisted surgical techniques and uses a trocar that can enter the skull through a very tiny incision. This methodology result shows that there is a significant improvement in the patient health with a slighter recuperating time period and more limited emergency clinics remain because of the little size of entry points.

Many examination endeavors have zeroed in on plans and improvements in regards to these careful robots, especially in these type of concentric cylinder controllers, a mix of nitinol (nickel-titanium) pre-curved flexible cylinders that can be broadened, shrank, and turned regarding one another, permitting the tip to explore too little and almost distant careful destinations [3, 4]. Utilizing this stage, little careful devices with end effectors, for example, a scissor, and grasper or camera that can be planned and measure up to the size of 2 mm and at the same time maintain their smoothness and power needed to remove brain tumors excluding skull open medical procedure [5].

Notwithstanding its mechanical advancement and advantages, there are exceptionally restricted haptics in particular material and sensation data being gotten by the specialists because of the controller of the automated frameworks. The trocar influence and the concentric cylinder framework occur a power applied to the device handle is not accurately meant for the instrument shaft and tip, where apparatus tissue connections happen [6]. This decreased reasonable power sensation which may miss the command over the tissue, due to this unexpected sudden injury and slippage is likely to occur. Thus, power criticism is needed to give instrument-tissue communication data to the specialists and to guarantee wellbeing and compelling activity.

In recent neurosurgeries, sources were applied in the careful instrument to the cerebrum tissue which was normally placed beneath in range of the hundred-factory Newton. For wound cuts, the middle power is around 10 mN to 50 mN, paying little heed to the brain area being controlled [7]. In addition, the middle power needed to withdraw a specific segment of the cerebrum is around 80 mN, which is lesser than the hundred-plant Newton scope induce an iatrogenic physical issue in intraventricular neurosurgeries [7]. Consequently, the tactile sensor along with high sensitivity along with few loads with the operation of the force feedback system significantly reduced the iatrogenic injuries. There are some high-goal, little, and adaptable material sensors that can practically the entirety of the transduction modes: piezoelectric, optical, inductive, capacitive, and piezoresistive [8].

Pyo et al studied The Carbon- NanoTube (CNT) using the PDMS composite along with four sensing elements to absorb the normal and shear forces performances. This type of sensor is able to sense the low range of force up to 500mN with higher repeatability of 2.0% deviation [9]. Schwartz et al. proposed the integrated micro structured PDMS dielectric with poly isoindigo bithiophene-siloxane semiconductor to design a capacitor sensor with a remarkable fast sensing response time of < 10ms, stability > 15,000 cycles, and pressure of 8.2 kPa [10]. Numerous test methods on different low power range material and weight sensors, a few of which attract attention to their application, especially in their endoscopic medical field. [11, 12]. Generally, Fiber Bragg Grating (FBG) sensors have been actualized to careful grasper and cardiovascular catheter plans to lead multi-directional power estimations [13, 14].

Li et al. proposed a miniature knock molded piezoelectric PVDF TrFE film for dynamic power detecting spiral catheter structure [15]. Arabagi et al.[16] reported the pressure detecting sensor with endoscopic 6.5-mm through cortical using piezoresistive PDMS-based eutectic gallium-indium (eGaIn) for trans cortical depression test. Kim et al. designed a capacitive based sensor with minimal cautious gripper for

typically low and shear force estimations [17–19]. In addition, Naidu et al.[20] comparatively studied both piezoresistive and capacitive weight sensors to monitor the palpation and to distinguish the tumor tissues. However, most of these optical, piezoelectric, piezoresistive, capacitive power sensors & power detecting resistor intended for endoscopic applications are bulky and defenseless to bowing, misalignment, and static detecting [21, 23].

In this research another detecting technique is proposed. This strategy utilizes the RI changes in 2D photonic precious stone detecting standard for separate the typical anomalous tissues in brain during a medical procedure. Ordinary and anomalous tissues in brain have distinctive refractive records. This sensor absolutely follows photonic crystal structures and standards. Tissues could be characterized optically.

2. Photonic Crystal Sensor

Developing interests have appeared over the most recent couple of years in the plan and enhancement of photonic crystal-based segments, for example, waveguides, lasers, splitters, strands. Photonic crystals have optical materials properties and are subject to changes in their refractive index periodically. In addition, the propagation of electromagnetic waves is prohibited for a particular frequency range and gives a promising device to control the progression of light in incorporated optical equipment. It also depends on the wavelength when the photons propagate either through the structure or not. The photonic crystals exhibit properties and are named as Photonic Band Gap (PBG). It also refused the propagation of light within the range of frequency. Increases the effective optical path and enhances the interaction between the gas and light-medium by using the photonic crystal during the slow-light regime. The use of photonic crystals for the design of biosensors in a variety of ways and use in medical applications is one of the most sought after in today's era.

There are few numerous strategies, such as the Transfer Matrix Method (TMM) [24], Finite Element Method (FEM) [25], Finite-Difference Time-Domain (FDTD) Method [26], and Plane Wave Expansion (PWE) method [27] are easily accessible to investigate the transmission spectra and dispersion behavior of PCs. Every method has a few unique advantages and disadvantages. Here are a few methods such as PWE and FDTD that are dominant according to their effectiveness; they are at the forefront of fulfilling the demands of PC-based devices.

In general, the theoretical analysis of PC structures was carried out initially by using the PWE method and indeed that the Eigen-modes within periodic structures reveal a superposition of a group of plane waves. Similarly, another method of approach is using numerical solutions of Maxwell’s equations to estimate both field distribution and transmission spectra through Finite-Difference Time-Domain (FDTD) method. In this research work, the propagation modes and band gap of the Photonic crystal structure were calculated by using the PWE methods, and however, the spectrum of power transmission was measured using the 2DFDTD methods [28]. Subsequently, the certain frequencies of electromagnetic waves during

the transmission are prohibited and few ranges of wavelengths also restricted during the propagation of light [29]. Here, the defect mechanism concept was used to manipulate the light propagation.

The ring resonator is used to improve the sensitivity of photonic crystals and in addition to that the line defects in the resonator act as a waveguide. Moreover, the resonant wavelength and the output power of the ring resonator can be changed based on the variation of the refractive index. By using Maxwell's electromagnetic Eq. (1), it is easy to prove that PC's functions are almost similar to the sensor [30–33].

$$\nabla \times \left[\frac{1}{\epsilon}\nabla \times H\right] = \left[\frac{\omega}{c}\right]^2 H \qquad (1)$$

Where C is the speed of light, ∈ is the permittivity, and H is the magnetic field and ω is the frequency of resonance. It is noted that the frequency varies whenever there is a change in the dielectric function. The analysis of the sensitivity performance of the structure is given by Eq. (2)

$$\text{Leff} = Q\lambda/2\pi n \qquad (2)$$

Where L_{eff} is named as effective interaction length, Q is the ring resonator quality factor, λ is the wavelength of the ring resonator, and n is the refractive index.

3. Materials And Methods

The most important consideration in the biomedical diagnosis is the refractive index (RI). It was found that the refractive index values of various benign and malignant tumors together with metastasis determined by an Abbe refractometer in the laboratory (34). They are different and depend on the percentage of water and protein/phospholipids. In general, resonances are normally more sensitive when certain changes occur.

Table 1
List of refractive index (RI) of the different brain tissues.

Tissues			Refractive index
Normal tissues		Gray matter	1.3951
		White matter	1.4121
		Cerebrospinal fluid	1.3333
Abnormal tissues	Lesions (injured tissues)	Wall of solid brain	1.3412
		Multi sclerosis	1.3425
		Oligodendroglioma	1.3531
	Tumors & Cancers	Low grade glioma	1.4320
		Medulloblastoma	1.4412
		Glioblastoma	1.4470
		Lymphoma	1.4591
		Metastasis	1.4833

Precise and quantitative amounts of water and solid contents like protein and phospholipids of a brain lesion can only be separated by using T1 or T2 relaxation time (35–39).The information about the refractive index of the normal and abnormal tissues is given in the Table1. Here, Abbe refractometer is used to determine the refractive index value of the biopsy tissues and homogenates.

4. Sensor Design

The figure shows that the biosensor which is based on Photonic crystal design consists of the hexagonal array of a circular rod placed in a background of air (RI = 1). In X and Z directions the number of rods in the hexagonal lattice is 30 and 33, respectively. The rod in the hexagonal lattice has a radius of 110 nm and subsequently, the distance between the two which was placed adjacent is 540 nm and named as a lattice constant which is denoted by a letter “a”. The circular structure of the silicon rod has a dielectric constant of 11.97 (refractive index $n = 3.46$).

The two hexagonal ring resonators of the sensor placed in this design and each of the rod radius are 110 nm. The radius of six rods, which are placed around the middle rod is 55nm. The radius of black encircling rod is 33.67nm.The biosensor has two ports as input and output ports, where ports are used at different wavelengths to analyze and propagate the optical signals. Figure 1 shows the schematic diagram of the biosensor with a hexagonal ring resonator used to identify the abnormal tissues.

The Photonic Band Gap (PBG) has significant focus recently due to its ability to control electromagnetic waves in three different directions. Here, the PBG is identified by using the plane wave expansion

technique. Figure 2 shows the band diagram of the PBG with dimension of 30x33 hexagonal lattices without defects.

The PC Structure has the normalized frequency is expressed as

$$\omega a/2\pi c = a/\lambda \qquad (3)$$

Where, a is the lattice constant of the crystal, ω is the angular frequency of the PC, c is the velocity of light in free space, and λ is the wavelength. The PBG in two TE modes at different wavelengths in the band diagram was in the range of 1224 nm to 1985 nm and 912 nm to 972 nm. The window of PBG ranging from 1224nm to 1985nm is most relevant and this effort counts with it.

Figure 2 also illustrated the proposed band diagram of a 30x33 hexagonal ring resonator after revealed the point defects as well as line defects. The obtained guided mode diagram clearly shows due to the incorporation of an elliptical shape ring resonator in the periodic structure, there is a propagation mode in the PBG region. Here, designed sensor with the line and point defects used to perform the analysis of the abnormal tissue. The 3D view of the hexagonal structure bio sensor is shown in Fig. 3. The size of the hexagonal structure biosensor is 16.2μm × 15.4 μm.

5. Results And Discussion

As the light signal passes through the elliptical shape of the resonator and propagates into the waveguide then the biosensor with a hexagonal ring resonator utilizes the power monitor at the output port of the sensor in order to measure the output signal power. The output response obtained in this is used to estimate the quality factor, resonant wavelength, and output power. Figure 4 clearly shows the normalized output power transmission spectrum of the proposed bio-sensor. The obtained simulation results show that the resonant wavelength of the proposed biosensor, output efficiency of the sensor, and Q factor at normal condition is 1544 nm, 100%, and 454, respectively.

Figures 5(a) and 5(b) shows the distribution of electric field of biosensors during the ON /OFF condition of resonance. When **λ** = 1544 nm then hexagonal ring resonator is ON, i.e. the input signal is associated with the input waveguide to the hexagonal ring resonator which produces the output as a waveguide. Similarly, the input signal is reflected back to the input source when the hexagonal ring resonator is in OFF condition (**λ** = 1548nm). The change in the equivalent resonant wavelength and change in the normalized transmission output power levels that occur in each brain tissue refractive index value which is filled background of circular rods instead of air. In addition, each spectrum represents the corresponding brain normal and abnormal tissues.

The resonant wavelength, refractive index, Q factor, and output efficiency for the corresponding brain tissues are given in the Table 2. Here, Metastasis cancer tissue has a significantly higher refractive index value than the other brain tissues as mentioned in the Table 2. The result obtained from the simulation

analysis of biosensor using hexagonal ring resonator is significantly more sufficient for real-time applications.

Table 2
Comparative various features of the various normal and abnormal brain tissues.

Name of the Various brain tissues	Refractive index	Resonant wavelength (nm)	Quality factor	Output efficiency (%)
Gray matter	1.3951	1695	565	97.14
White matter	1.4121	1717	505	96.23
Cerebrospinal fluid	1.3333	1648	549	97.74
Wall of solid brain	1.3412	1656	502	99.61
Multi sclerosis	1.3425	1662	573	98.13
Oligodendroglioma	1.3531	1671	522	98.72
Low grade glioma	1.4320	1730	494	98.31
Medulloblastoma	1.4412	1743	562	96.37
Glioblastoma	1.4470	1762	452	99.82
Lymphoma	1.4591	1769	432	97.75
Metastasis	1.4833	1794	427	97.77

The few characteristics, names of the different brain tissues, and their normal values are clearly given in Table 2. Brain tissues can be classified in any patient during MIS and do extensive research to diagnosis their brain. Each characteristic of the brain tissues are identified and its value is compared with the given Table 2. At last, the exact abnormal tissue location is identified more accurately within a minimal amount of time. From the table, it can be seen that some of the tissues have a higher refractive index than the others. This happens due to the fact that the different physical, chemical, and biological properties of the normal and abnormal brain tissues.

Figure 6.Variation of resonant wavelength (nm) with respect to the refractive index of the brain tissues.

In order to evaluate the effectiveness of the results are compared the proposed works with the various research works as shown in the figure.7

6. Conclusions

In this research work was carried out to investigate the sensing characteristics of the two dimensional photonic crystal based biosensor. Here, the two-dimensional photonic crystals are used to design the

biosensor along with the hexagonal lattice of the circular rods.. The biosensor operates within the range of 1544 nm to 1800 nm wavelength which is useful in analyzing the Q factor, refractive index, and biosensor output power. The brain tissues have some range of RI values and whether it is a normal or abnormal tissue in the brain depending on the increments or diminished levels. By utilizing the planned sensor, these tissues can be distinguished the tissues during MIS of brain. Subsequently, this work will be extremely attractive for early diagnosis of brain tumors and cancer.

Declarations

Ethics Approval and Consent to Participate Not Applicable

Consent for Publication

I give my consent for the publication of identifiable details, which can include images, graphs, simulation results within the text to be published in this journal and article. I have discussed this consent with my coauthor.

Availability of Data and Materials

The data that support the findings of this study are available from the corresponding author upon reasonable request.

Competing Interest Not Applicable

Funding

NIL: No special funding agency contributes with my research.

Authors Contribution

A.Asuvaran: Writing - original draft, Designing of sensor

G.Elatharasan: Methodology, Investigation, Writing - review & editing.

Acknowledgements:

The entire research work is carried out in University College Of Engineering, Pattukkottai, which is one of the constituent college of Anna University, Chennai

Disclosure of Potential Conflicts of Interest

We declare all this manuscript is original, has not been published before and is not current being considered for publication elsewhere. We know of no conflict of interest associated with this Publication, and there has been no significant financial support for this work that could have influenced its outcome.

As a corresponding author, I confirm that the manuscript has been read and approved for the submission by all the co-authors.

Research Involving Human Participants and/or Animals

Not Applicable

Informed Consent

Not Applicable

References

1. Ostrom QT, Gittleman H, Fulop J, Liu M, Blanda R, Kromer C, *etal.*, "CBTRUS statistical report: primary brain and central nervous system tumors diagnosed in the United States in 2008–2012," *Neuro.Oncol.*, vol. 17 Suppl 4, pp. iv1-iv62, Oct 2015.DOI: 10.1093/neuonc/not151
2. Udaka YT, Packer RJ (Aug 2018) "Pediatric brain tumors". Neurol Clin 36:533–556. DOI:10.1007/s11060-020-03437-4
3. Lee DY, Kim J, Kim JS, Baek C, Noh G, Kim DN et al (Dec 2015) "Anisotropic patterning to reduce instability of concentric-tube robots". IEEE Trans Robot 31:1311–1323. DOI:10.1109/TRO.2015.2481283
4. Kim J, Choi W-Y, Kang S, Kim C, Cho K-J (2019) Continuously variable stiffness mechanism using non uniform patterns on coaxial tubes for continuum microsurgical robot. IEEE Trans Robot. DOI:10.1109/TRO.2019.2931480
5. Forbrigger C, Lim A, Onaizah O, Salmanipour S, Looi T, Drake J et al (Apr 2019) "Cable-less, magnetically driven forceps for minimally invasive surgery". IEEE Robot Autom Lett 4:1202–1207. DOI:10.1109/LRA.2019.2894504
6. Trejos AL, Patel RV, Naish MD, "Force sensing and its application in minimally invasive surgery and therapy: a survey," *Proc.Inst. Mech. Eng. C*, vol. 224, pp. 1435–1454, 2010.DOI: 10.1243/09544062JMES1917
7. Marcus HJ, Zareinia K, Gan LS, Yang FW, Lama S, Yang GZ,*et al.* (Jun 2014) "Forces exerted during micro neurosurgery: a cadaver study". IntJ Med Robot 10:251–256. doi:10.1002/rcs.1568
8. Chortos A, Liu J, Bao ZA (Sep 2016) "Pursuing prosthetic electronic skin. "*Nat Mater* 15:937–950. DOI:10.1038/nmat4671
9. Pyo S, Lee JI, Kim MO, Chung T, Oh Y, Lim SC et al, "Development of a flexible three-axis tactile sensor based on screen printed carbon nanotube-polymer composite," J Micro mech Microeng,24, Jul 2014.DOI:10.1088/0960-1317/24/7/075012
10. Schwartz G, Tee BCK, Mei JG, Appleton AL, Kim DH, H. L.Wang, *et al.*, "Flexible polymer transistors with high pressure sensitivity for application in electronic skin and health monitoring" Nat Commun,4, May 2013.DOI:10.1038/ncomms2832

11. Dai Y, Xue Y, Zhang JX (Oct 2016) Milling state identification based on vibration sense of a robotic surgical system. IEEE Trans IndElectron 63:6184–6193. DOI:10.1109/TIE.2016.2574981
12. Liang WY, Ma J, Tan KK, "Contact force control on soft membrane for an ear surgical device," in IEEE Transactions on Industrial Electronics, vol. 65, no. 12, pp. 9593–9603, Dec. 2018, DOI:10.1109/TIE.2018.2818647
13. Zhang T, Chen B, Zuo S (2021) "A Novel 3-DOF Force Sensing Micro needle with Integrated Fiber Bragg Grating for Microsurgery". IEEE Trans Industr Electron. DOI:10.1109/TIE.2021.3055173
14. Ferraro D et al (2021) "Implantable Fiber Bragg Grating sensor for continuous heart activity monitoring: ex-vivo and in-vivo validation". in IEEE Sensors Journal. doi:10.1109/JSEN.2021.3056530
15. Li A, Lee S, Gorton A, Schulz MJ, Ahn CH, "Dome or bump shaped PVDF-TrFE films developed with a new mold-transfer method for flexible tactile sensors," *Proceedings of the IEEE Twentieth Annual International Conference on Micro Electro Mechanical Systems, Vols 1and 2*, pp. 578-+, 2007.DOI: 10.1109/MEMSYS.2007.4433104
16. V.Arabagi O, Felfoul AH, Gosline RJ, Wood, Dupont PE (2016) Biocompatible pressure sensing skins for minimally invasive surgical instruments. IEEE Sensors J 16(Mar 1):1294–1303. DOI:10.1109/JSEN.2015.2498481
17. Kim U, Lee DH, Yoon WJ, Hannaford B, Choi HR (Oct 2015) Force sensor integrated surgical forceps for minimally invasive robotic surgery. IEEE Trans Robot 31:1214–1224. DOI:10.1109/TRO.2015.2473515
18. Kim U, Kim YB, Seok DY, So J, Choi HR (Mar 2018) "A surgical palpation probe with 6-axis force/torque sensing capability for minimally invasive surgery". IEEE Trans Ind Electron 65:2755–2765. DOI:10.1109/tie.2017.2739681
19. Kim U, Kim YB, So J, Seok D, Choi HR, "Sensorized Surgical Forceps for Robotic-Assisted Minimally Invasive Surgery," in IEEE Transactions on Industrial Electronics, vol. 65, no. 12, pp. 9604–9613, Dec. 2018, doi: 10.1109/TIE.2018.2821626
20. Naidu AS, Patel RV, Naish MD (Feb 2017) Low-cost disposable tactile sensors for palpation in minimally invasive surgery. IEEE/ASMETrans Mechatron 22:127–137. DOI:10.1109/TMECH.2016.2623743
21. Zhou D, Tadano K, Haraguchi D (2020) Motion Control and External Force Estimation of a Pneumatically Driven Multi-DOF Robotic Forceps. Appl Sci 10:3679. doi:10.3390/app10113679
22. Chi A, Sun XG, Xue N, Li T, Liu C, "Recent progress in Technologies for tactile sensors," *Sensors*, vol. 18, Apr 2018, DOI: 10.3390/s18040948
23. Chen T et al., "Novel, Flexible and Ultra-thin Pressure Feedback Sensor for Miniaturized Intra-ventricular Neurosurgery Robotic Tools," in IEEE Transactions on Industrial Electronics, April 2020, doi: 10.1109/TIE.2020.2984427
24. Robinson S, Nakkeeran R (2011) PCRR based band pass filter for C and L + U bands of ITU T G.694.2 CWDM systems. Optics Photonics Journal 1(3):142–149. DOI:10.4236/opj.2011.13024

25. Pelosi G, Coccioli R, Selleri S, “Quick finite elements for electromagnetic waves”. Boston, London, England: Artech House (1997) 1–289.DOI: 10.1109/MEI.1999.793831
26. A.Taflove and Hagness SC (2005) Computational electrodynamics: the finite-difference time-domain method. Artech House, Boston, pp 1–1038
27. Johnson SG, Joannopoulos JD (2000) Block-iterative frequency domain methods for Maxwell's equation in a plane wave basis. Opt Express 11(3):173–190. DOI:10.1364/OE.8.000173
28. Guo S, Alloin S (2003) Simple plane wave implementation for photonic crystal calculation. Opt Express 11(2):167–175. DOI:10.1364/OE.11.000167
29. Scarmozzino R, Gopinath A, Pregla R, Helfert S (2000) Numerical techniques for modeling guided-wave photonic devices. IEEE J Sel Top Quantum Electron 6(1):150–162. DOI:10.1109/2944.826883
30. Arunkumar R, Suaganya T, Robinson S (2019) Design and Analysis of 2D Photonic Crystal Based Biosensor to Detect Different Blood Components. Photonic Sens 9:69–77. DOI:10.1007/s13320-018-0479-8
31. Ajey SS, Bhanumathi HR, Srikanth PC et al (2020) Highly sensitive photonic crystal based biosensor for Bacillus cereus. Int j inf Techno 12:1393–1402. DOI:/10.1007/s41870-020-00507-8
32. Rakshit BiswasU (2020) J.K. “Detection and analysis of hemoglobin concentration in blood with the help of photonic crystal based micro ring resonator structure”. Opt Quant Electron 52:449. DOI:10.1007/s11082-020-02566-4
33. Akahane Y, Asano T, Song BS, Noda S (2003) High-Q photonic nano cavity in a two dimensional photonic crystal. Nature 425:944–947. DOI:10.1364/ACPC.2017.Su4F.2
34. Luu TBiswas,T; “In vivo MR Measurement of Refractive Index, Relative Water Content and T2 Relaxation time of Various Brainlesions With Clinical Application to Discriminate Brain Lesions ”The Internet Journal of Radiology, Volume 13 ,Number 1, 2009,DOI:10.5580/1483
35. Joonmi O, Eric TH, Danie P, Nelson SJ (2006) Measurement of in-vivo multi-component T2 relaxation times for brain tissue using multi-sliceT2 prep at 1.5 and 3T. JMRI 24:33–43. DOI:10.1016/j.mri.2005.10.016
36. Graham SJ, Bronskill MJ (1996) MR measurement of relative water content and multi component T2 relaxation in human breast. Magn Reson Med 35:706–715. DOI:10.1002/mrm.1910350512
37. Moffat B, Pope J (2002) The interpretation of multi-exponential water proton transverse relaxation in the human and porcine eye lens. Magnetic Resonance imaging 20:83–93. DOI:10.1016/S0730-725X(02)00481-2
38. Grossman RI, Gomori JM, Ramer Kn, Lexa FJ (1994) SchnallMD. “Magnetization Transfer: Theory and Clinical Application in Neuro radiology”. Radio graphics 14:279–290. DOI:10.1148/radiographics.14.2.8190954
39. Papanikolaou N, Maniatis V, Pappas J, Roussakis A, Efthimiadou R, AndreouJ (2002) Biexponential T2 Relaxation Time Analysis of the Brain: Correlation with Magnetization Transfer Ratio. InvestRadiol 37:363–367. DOI:10.1097/00004424-200207000-00001

40. Radhouene M, Chhipa MK, Najjar M, S.Robinson, and Suthar B (2017) Novel design of ring resonator based temperature sensor using photonics technology. Photonic Sensors 7(4):1–6. https://doi.org/10.1007/s13320-018-0479-8
41. Mai TT, Hsiao FL, Lee CK, Xiang WF, C. C.Chen, and Choi WK (2010) Optimization and comparison of photonic crystal resonators for silicon micro cantilever sensors. Sensors Actuators A: Physical 165:16–25. https://doi.org/10.1016/j.sna.2010.01.006
42. Li B, Lee CK (2011) NEMS diaphragm sensors integrated with triple-nano-ring resonator. Sensors Actuators A: Physical 172:61–68. https://doi.org/10.1016/j.sna.2011.02.028
43. Sreenivasulu T, Rao V, Badrinarayana T, Hegde GK, Srinivas T (2018) Photonic crystal ring resonator based force sensor: design and analysis. Optik 155:111–120. https://doi.org/10.1016/j.ijleo.2017.11.040
44. Olyaee S, Bahabady AM (2014) Two-curve-shaped biosensor using photonic crystal nano-ring resonators. Journal of Nanostructures 4:303–308. DOI:10.7508/JNS.2014.03.007
45. Huang LJ, Tian HP, Yang DQ, Zhou J, Liu Q, Zhang P et al (2014) Optimization of figure of merit in label-free biochemical sensors by designing a ring defect coupled resonator. Opt Commun 332:42–49. https://doi.org/10.1016/j.optcom.2014.06.033
46. Olyaee S, Bahabady AM, “Designing a novel photonic crystal nano-ring resonator for biosensor application,” Optical Quantum Electronics, 2015, 1881–1888. https://doi.org/10.1007/s11082-014-0053-6
47. Harhouz A, Hocini A (2015) Design of high-sensitive biosensor based on cavity- waveguides coupling in 2D photonic crystal. Journal of Electro magnetic Wave Applications 29(5):659–667. https://doi.org/10.1080/09205071.2015.1012597
48. Hocini A, Harhouz A (2016) Modeling and analysis of the temperature sensitivity in two dimensional photonic crystal micro cavity. J Nanophotonics 10(1):016007–016010. https://doi.org/10.1117/1.JNP.10.016007
49. Arafa S, Bouchemat M, Bouchemat T, A.Benmerkhi, and Hocini A (2017) Infiltrated photonic crystal cavity as a highly sensitive platform for glucose concentration detection. Opt Commun 384:93–100. https://doi.org/10.1016/j.optcom.2016.10.019

Figures

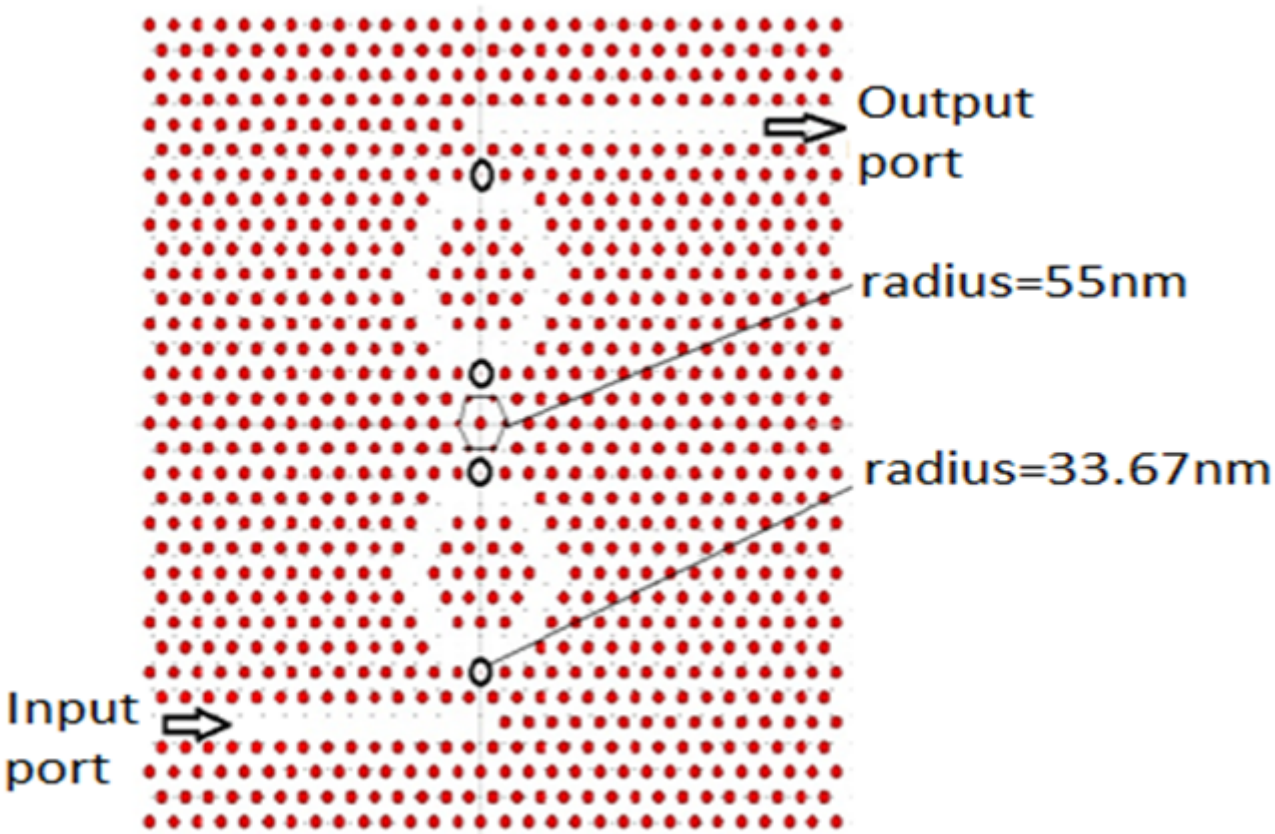

Figure 1

Schematic diagram of the biosensor with a hexagonal ring resonator

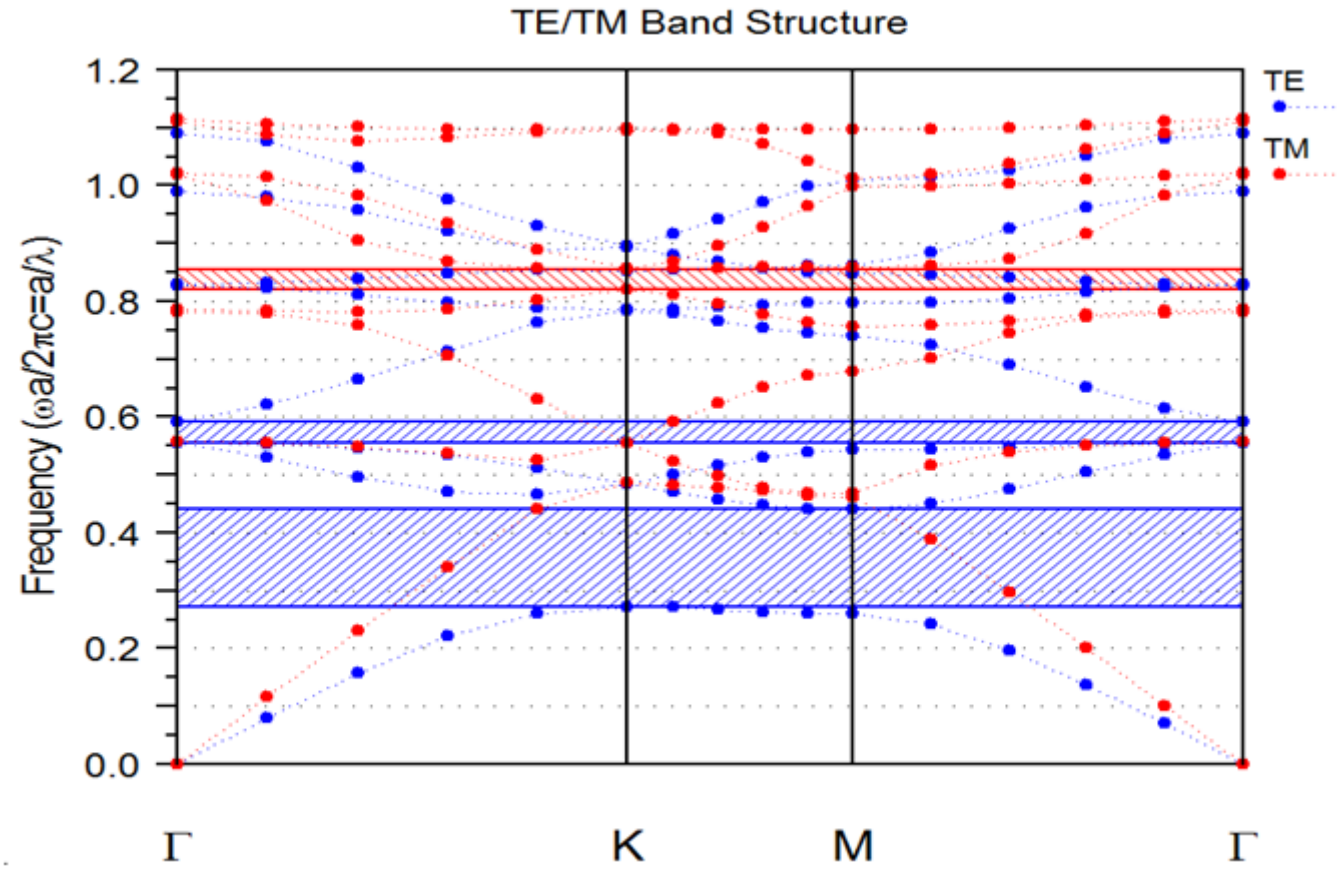

Figure 2

Band diagram for circular rods in 30 × 33 hexagonal lattice with line and point defects.

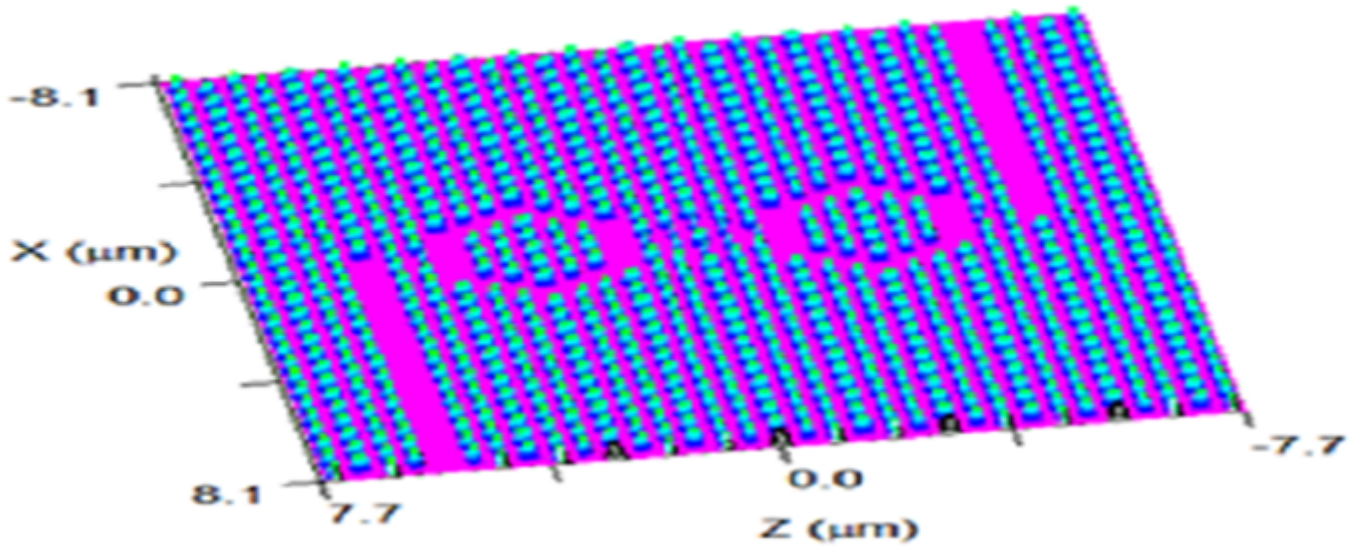

Figure 3

Three dimensions of the biosensor with a hexagonal ring resonator.

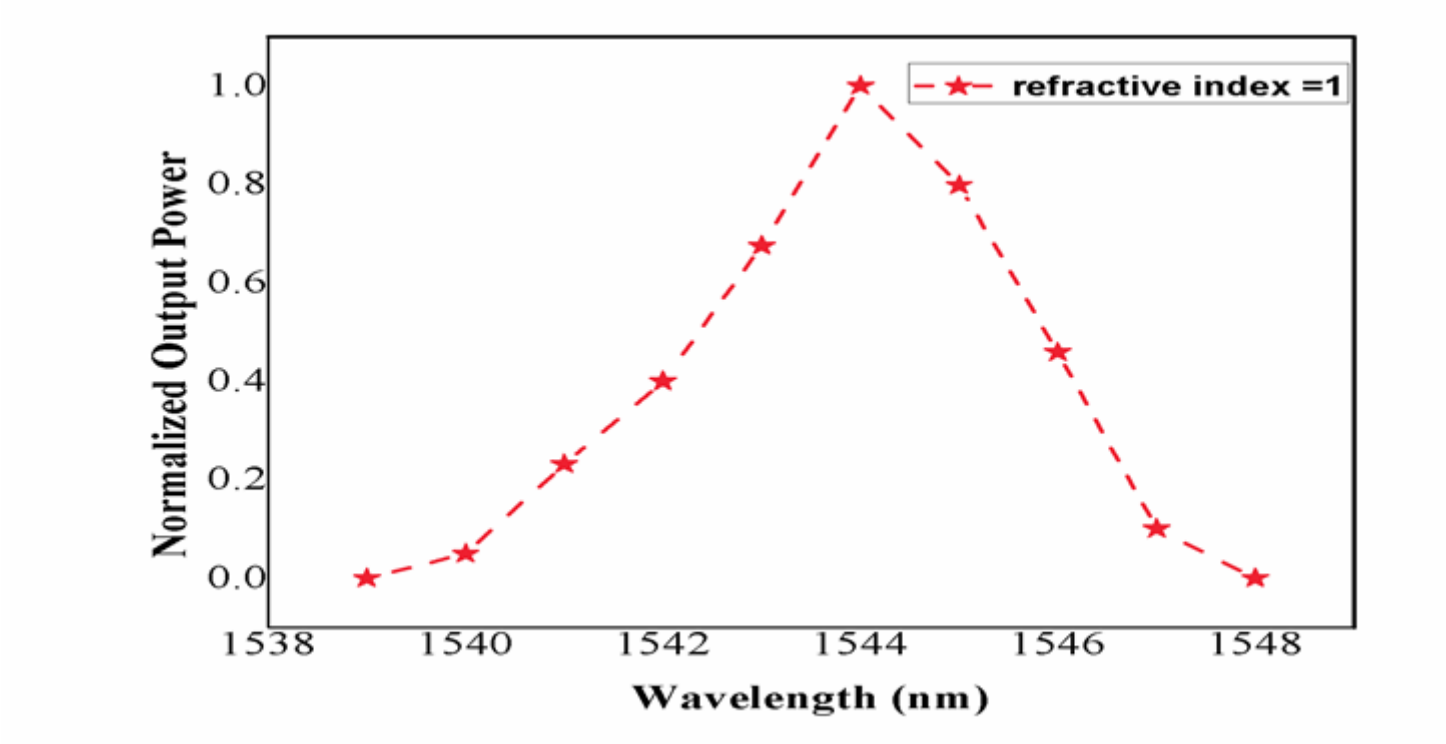

Figure 4

Graph between Normalized Output power and wavelength for the proposed biosensor

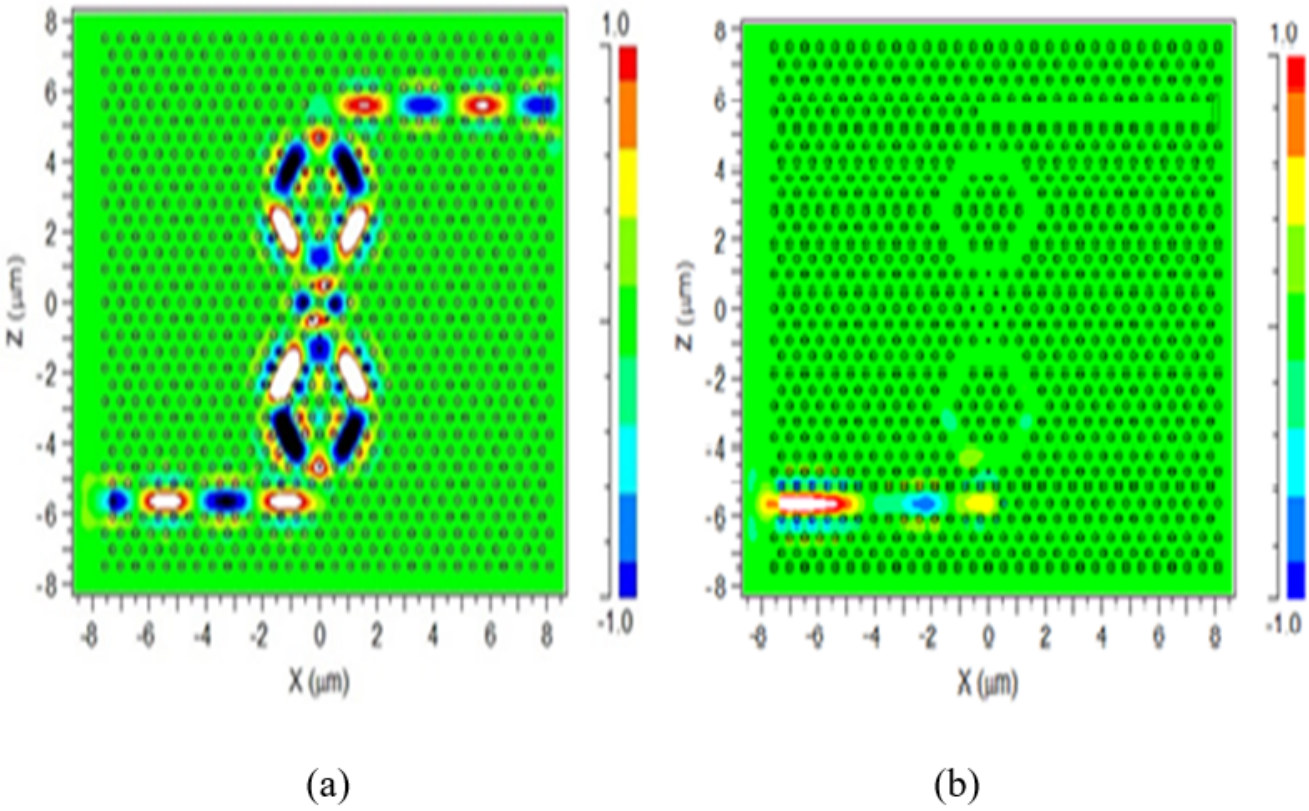

Figure 5

Wave propagation of the proposed bio sensor at (a) ON resonance (λ= 1544 nm) and (b) OFF resonance (λ= 1548 nm).

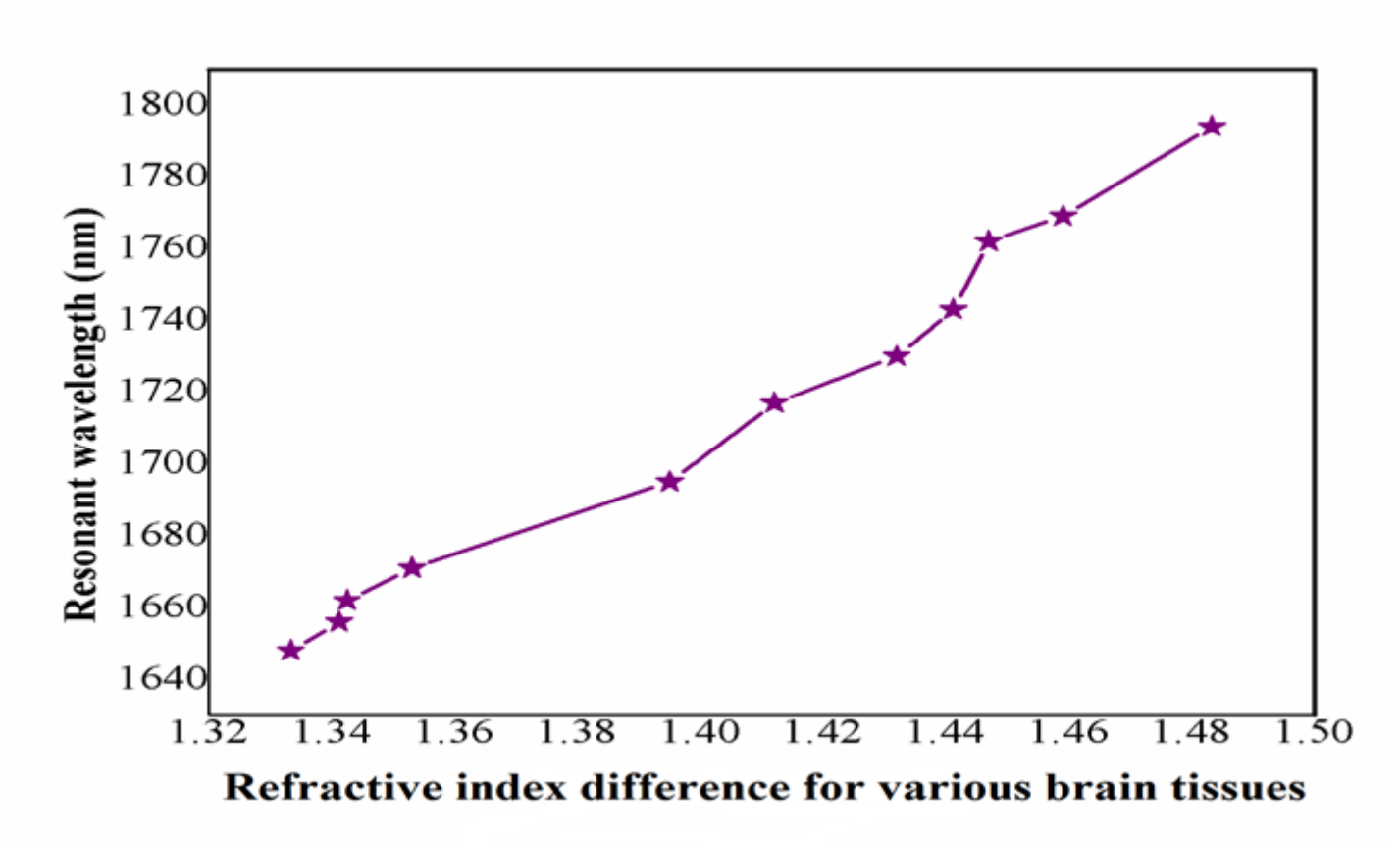

Figure 6

Variation of resonant wavelength (nm) with respect to the refractive index of the brain tissues.

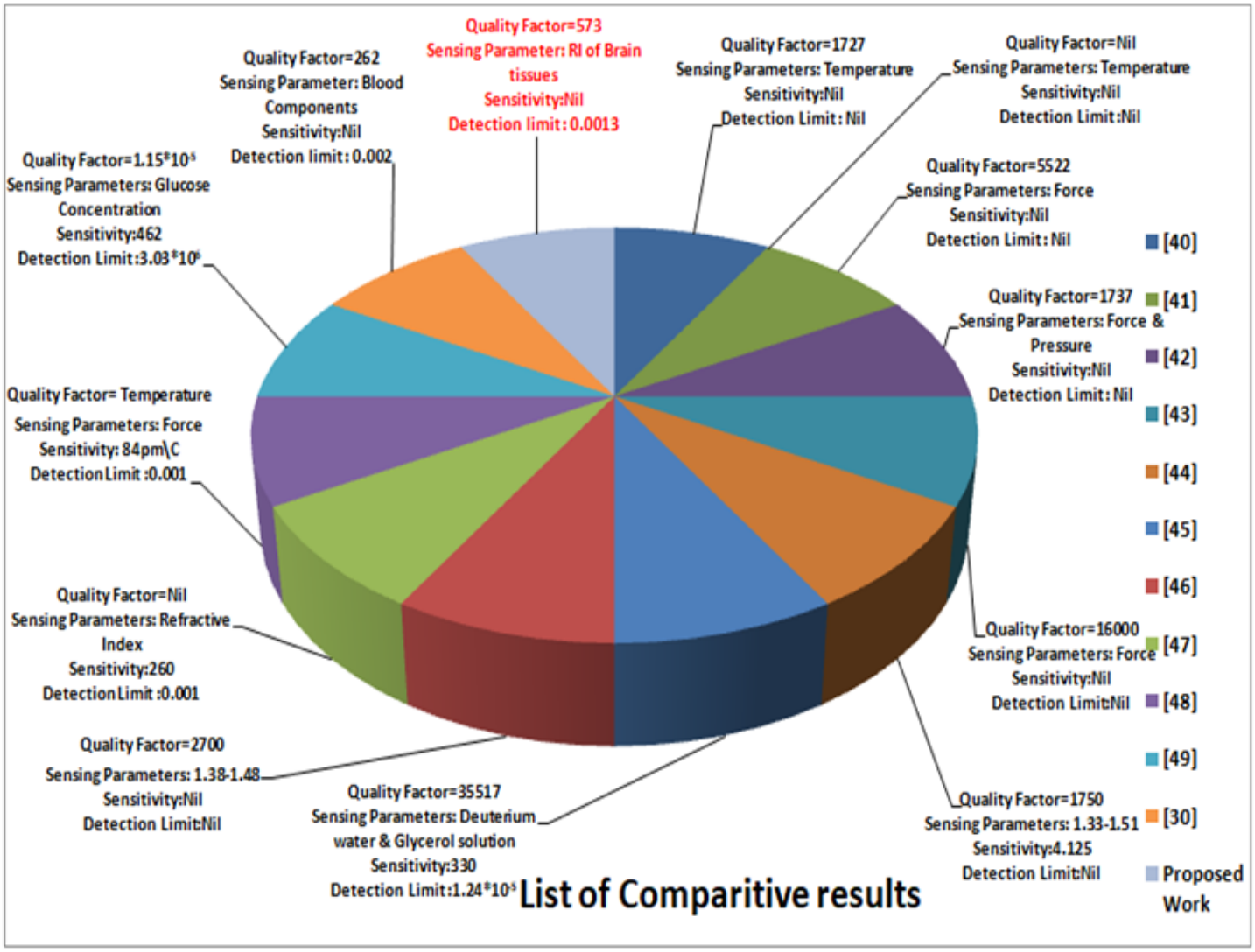

Figure 7

Comparison of various research works with the proposed work.